

# ***IN-SITU* RESISTANCE CHARACTERIZATION DURING CURE PROGRESSION OF A CONDUCTIVE ADHESIVE**

Geoff Rivers<sup>1</sup>, Pearl Lee-Sullivan<sup>1</sup>, and Boxin Zhao<sup>2</sup>

<sup>1</sup> Department of Mechanical and Mechatronics Engineering

<sup>2</sup> Department of Chemical Engineering  
University of Waterloo, Waterloo, Ontario, Canada

Alex Chen

Celestica Inc. Toronto, Ontario, Canada

John Persic and Robert Lyn

Microbonds Inc, Toronto, Ontario, Canada

## **ABSTRACT**

Methodology and equipment have been developed for *in-situ* characterization of electrical resistance of thermosetting conductive adhesives during the cure process. It has long been known that conductive adhesives have poor conductivity while in their uncured state, and develop conductivity as the polymer cures and allows the establishment of a conductive filler network. In this paper, we will present a novel method for obtaining sheet resistance measurements of a conductive thermosetting composite under controlled heating conditions, during the crosslinking process. *In-situ* resistance measurements are compared with calorimetry performed under the same heating conditions, allowing direct correlation. As a result, unexpected and previously unreported behavior during the final stages of cure has been identified: a significant and temporary increase in electrical resistance mid-cure, after the resistance has begun decreasing, contrary to the power-law reduction as cure progresses. The dynamics of this process, and the final adhesive properties, are not yet understood. As such, this new *in-situ* technique will be instrumental for ongoing work to improve the conductivity of adhesives at lower filler contents and costs.

Keywords: Conductive adhesive, composite, conductivity, cure, thermoset

## **INTRODUCTION**

### **Background**

Conductive adhesive composites have long been used as a low temperature alternative to metallic soldering materials<sup>1</sup>. Recently, much work has been directed at the development of nanocomposites and hybrid-nanocomposite adhesives, to reduce cost and improve strength by reducing the total filler content, and improve the conductivity<sup>2</sup>. The use of nanoparticles opens the door to resistance reductions at low filler content through geometry effects (such as high aspect ratios and inter-particle bridging) and through the ability of metallic nanoparticles to undergo sintering and joining at low temperatures, reducing contact resistance.

Thermosetting conductive adhesives, such as those based on epoxy, solidify during chemical curing which shrinks the composite volume. It is generally believed that during this process polymer movement away from spaces between filler particles and the contraction of the polymer establishes contact within the filler network, enabling it to be conductive<sup>3</sup>. As such, the resistance of a thermosetting conductive adhesive is expected to reduce throughout the cure process.

This process is poorly characterized in the scientific literature, typically studied by *ex-situ* “before and after” resistance testing of partially cured composites<sup>1, 3-7</sup>. However the development of the properties during cure is complex, and often sensitive to the exact time-temperature conditions<sup>8</sup>. Also, contemporary nanocomposites often take advantage of low-temperature sintering between metallic nanofillers during the polymer cure, to reduce internal contact resistance in the filler network and improve composite conductivity<sup>9-16</sup>. Those processes are dependent on filler proximity and inter-filler barriers, and therefore would be expected to be influenced by the behavior during polymeric cure<sup>1, 9, 15</sup>.

Combined with a desire to reduce required process cycle times, it becomes apparent that there is a need for greater detail in the analysis of the changing electrical resistance of composite conductive adhesives under process conditions. Currently the open literature contains only limited *in-situ* and real-time investigations into this process<sup>8, 17-20</sup>.

### **State Of The Art**

A review of the recent open literature demonstrates the substantial need to improve the capacity to investigate the conductivity development in an *in-situ* method. A Compendex search of the terms “conductive adhesive”, “nano”, and “cure” between the years of 2006 and the present was used.

Of the 1052 papers found studying conductive adhesive composites containing nanomaterials, only 105 also studied

the cure behaviour in detail. Dropping “nano” from the search, only 8 papers were found in that time range to have studied the effect of cure on the changing resistance of conductive adhesives in detail<sup>5-8, 17, 19, 20</sup>. Three additional and highly influential publications on this topic can be found from 2002, 2001, and 1996, and should be noted here<sup>1, 4, 5</sup>. Of the 8 publications since 2006, 5 utilized in-situ methods<sup>8, 17-20</sup>, while the rest relied on before-and-after ex-situ measurements. And, of those 6 in-situ papers, only 2 characterized the changing resistance of curing conductive adhesives that contained nanomaterials<sup>19, 20</sup>. Both of those papers were published by a single group of researchers in 2015, concurrent with the ongoing studies of the authors. Thus, in the last 10 years, in-situ analysis of the changing conductivity of a thermosetting nanocomposites adhesive constitutes approximately 0.2% of all nanocomposites conductive adhesive publications.

Thus it can be seen that although knowledge of this mechanism’s existence has been available for decades, contemporary work into the details and complexities of the process are scarce. Likewise, little work has been completed with contemporary nanofillers, which are rapidly evolving.

In this work, we present a new approach for in-situ electrical resistance measurement of thermosetting composite conductive adhesives. We use a micro-particle silver filled adhesive resin to demonstrate proof-of-concept of its operation, under conditions that allows correlation of temperature, conversion, and resistance. In doing so, we present preliminary results of as yet unreported cure behavior during the final stages of cure.

## METHODS

The progression of cure conversion was measured as a function of changing resistance of a conductive microcomposite using two techniques: (i) a Modulated Temperature Differential Scanning Calorimetry (MTDSC) instrument and (ii) a custom-built 4-wire resistance measurement probe set-up

The composite consisted of 60wt% silver 10 $\mu$ m microflake and a widely used bisphenol A diglycidyl ether epoxy matrix binder, hardened by 13 PHR triethylenetetramine. Mixing was performed in a planetary centrifugal mixer, mixing silver flake for 5 minutes at 2000 RPM, followed by cooling to room temperature and mixing of hardener for 5 min at 2000 RPM. Composite silver content was selected as a control for later low-filler content hybrid nanocomposites.

MTDSC was performed in a TA Instruments TA DSC 2920, heated from room temperature to 175°C, modulating at +/- 0.159°C every 60 seconds, with an underlying heating rate of 1°C/min. This obtains non-reversing heat flow and the reversing heat capacity throughout the heating condition. Non-reversing heat flow was normalized to specimen mass (typically 12-16 mg, recorded individually), and the baseline subtracted. Non-reversing heat flow amplitude was

considered proportional to the rate of curing, and developed enthalpy at each incremental temperature  $T_i$  was calculated by integration between  $T=0$  and  $T=T_i$ . Incremental conversion ( $\alpha_i$ ) was calculated as incremental developed entropy ( $H_i$ ) divided by total developed entropy ( $H_\infty$ )

Resistance throughout cure progression was measured *in-situ* using a custom-designed mold with inlaid probe, described below in greater detail. In general, a 4-wire resistance method was used, measured by a source-meter controlled and recorded by a custom data acquisition program. Measurements were made every 15 seconds.

## Details Of Resistance Probe Design

The current design, presented in Figures 1a-c, was developed utilizing the derivations of 4-Wire Kelvin resistance measurements for various specimen geometries, as discussed by Schroder<sup>21</sup>.

The typical procedure reported in the in-situ and ex-situ literature is 4-wire resistance measurement. This has distinct advantages over 2-wire resistance methods: the removal of the lead resistance from the measurement, and often greater sensitivity due to the voltage and current being applied and read separately. However, there are a variety of ways 4-wire measurements can be performed. The literature examples typically performed their measurement on a

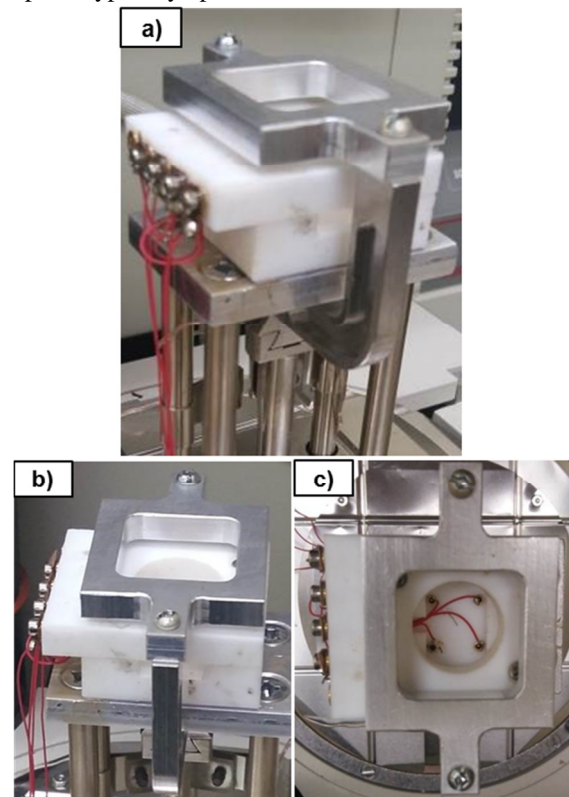


Figure 1 - Schematics and photos of the assembled mold-probe, installed in the DMA. a) Isometric view, b) Side view, c) top view, showing “trouble-shooting port” and the wired connections between external leads and mounted pin terminals.

rectangular specimen of composite spread onto a surface, such as glass, and then scraped to size using a doctor's blade<sup>8, 17-20</sup>. Most papers reported using a co-linear probe, though some quoted a two contact-point 4-wire probe, or some similar variant<sup>8, 17-20</sup>. Resistivity measurements were typically calculated using Equation 1, where  $R_L$  represents the square-resistance, or "sheet" resistance, and  $t$  represents the specimen thickness<sup>8, 17-21</sup>. It would appear, based on the numbers given, that most in-situ specimens were placed in a pre-heated chamber and allowed to heat in uncontrolled "spiked" heating to an isothermal temperature, rather than following a controlled heating rate.

$$\rho = R_L t \quad \text{Eq. 1}$$

$$R_L = (V_{1,2}/I_{3,4})(W/L) \quad \text{Eq. 2}$$

One notable concern is the calculation of  $R_L$  from  $V/I$  observations. Sheet resistance in the literature is typically obtained by Equation 2, where the specimen geometry is factored out by width  $W$  and length  $L$ <sup>21</sup>. However, this is the simplified solution, and intended for specialized circumstances, including specimens significantly larger than the probe<sup>21</sup>. Correction factors must be applied to the calculation of  $R_L$ , to account for the specimen geometry in relation to the probe geometry and placement<sup>21</sup>. This is especially true in the case of rectangular specimens that are measured using probes where each lead is a point-contact<sup>21</sup>. Co-linear probes are an industry standard due to their applicability to the resistance mapping of silicon wafers, and thus their availability<sup>21</sup>. However, Equation 2 is not applicable to co-linear probes, and the correction factors for co-linear probes are especially sensitive to the placement and relative size of the probe on the specimen, producing a source of error when the specimens are not significantly larger than the probe<sup>21</sup>. The correction factors used in the reviewed literature studies were not reported, and precise measurements would be required for their calculation.

We designed a reusable mold with a built-in 4-wire resistance probe that has been designed to obtain as simple and constant a correction factor as possible. For reusability, the mold is constructed of Teflon, preventing adhesion of the cured composite. In addition to its low-adhesion surface, Teflon is resistant to temperatures above 200°C, is electrically insulating, easily machined, and inexpensive. The contact components of the probe are low-cost standard gold-plated beryllium-copper PCB interconnect pins and sockets. This allows the pins to be imbedded and permanently cured into the sample, providing good electrical contact, then removed from the probe and replaced for the next specimen.

Instead of a rectangular specimen and a co-linear probe, the permanent mold geometry allowed the selection of a special case in the general 4-wire theory: a square specimen with the probe contacts located in the corners. This is shown in Figure 2. This sets  $W/L$  to unity, removing it from the equation, and links the probe placement and geometry to the specimen size, removing the need for placement and

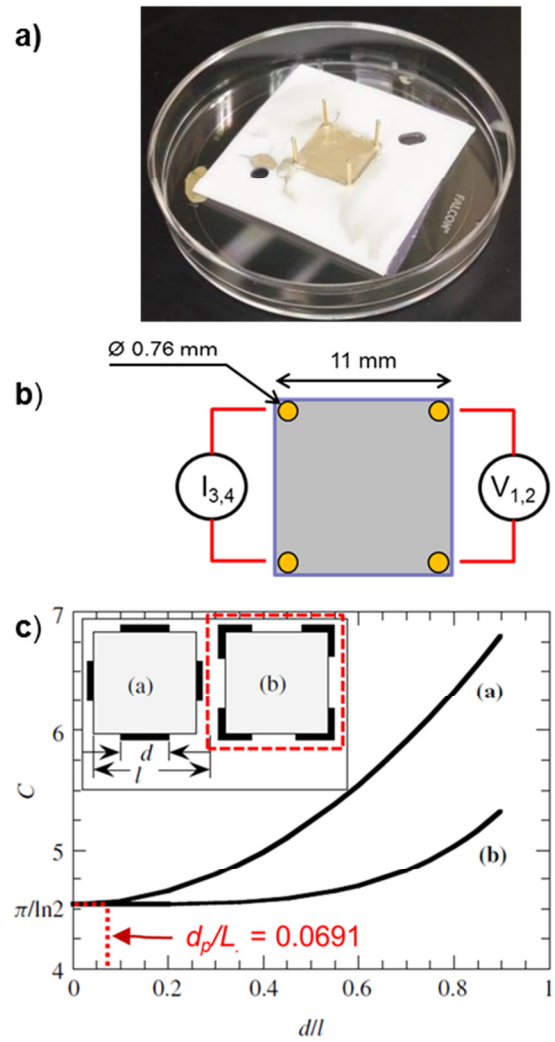


Figure 2 - a) specimen removed from the main mold block after resistance-monitored curing, encased by the white, 0.5mm thick teflon shape-mask. b) Top-down schematic of specimen. Gold represents contact pins, seen embedded in a). c) Correction factor vs  $d_p/L$  ratio, with applicable value marked in red. Adapted from reference<sup>21</sup>.

current-confinement correction factors. The only remaining correction factor needed is dependent on the ratio of the length of the specimen side ( $L$ ) to the diameter of the contact probe ( $d_p$ ). So long as the ratio  $d_p/L$  is less than 0.2, the correction factor is constant at  $C = \pi/\ln(2)$ , as seen in Figure 2c. The specimen dimensions are 11 mm square, and 0.5mm thick, and so the selected interconnect pins give a  $d_p/L$  ratio of 0.069, and therefore are well inside the linear regime of the correction factor. This also makes the required sample volume only 60.5 $\mu$ L. The use of a mold also allows for a more consistent and repeatable specimen thickness, giving this design a characteristic equation of:

$$\rho = (0.05)R_L = \left(\frac{0.05 \pi}{\ln 2}\right)(V_{1,2}/I_{3,4}) \quad \text{Eq. 3}$$

Experiments were completed using a source meter in auto-ranging mode, and the plots of sensitivity vs range for this probe's resistivity is plotted in Figure 3. In heating, the

Teflon expands faster than the beryllium-copper interconnects, and so when heated during an experiment  $d_p/L$  is reduced, ensuring that the correction factor remains valid throughout the operating temperature range, up to 200°C.

The spiked heating evident in the literature is effective for isothermal studies, as it represents the most rapid approach to the target temperature without overshooting. However, there are two major limitations to spiked heating. The first is that, due to the reaction kinetics, thermal history in the early stages of cure is very influential to the resulting cure behaviour and resulting polymer network. Since the spiked heating of a typical resistance sample and a DSC specimen will not be the same. This can lead to difficulty in estimating the actual degree of conversion of the resistance specimen, or comparing the two specimens' properties. Further, without controlled continuous heating, it is not possible to perform kinetics and low-heating rate work, which prevents the observation of possibly significant pieces of cure behaviour.

Our mold-probe was specifically designed for mounting onto a Dynamic Mechanical Analyser (DMA) instrument. Although the DMA cannot be used for mechanical analysis of the specimen with the current design, its furnace can match the heating programs and conditions that can be applied by the DSC, allowing both the DSC and resistance specimens to more accurately match one another's thermal histories, and allowing low-rate heating experiments.

In each test, we split a batch of uncured composite, one part for dispensing DSC specimens and the other, for casting resistance specimens. These are then stored at low temperature (at least 40°C below the initial uncured glass transition temperature) to prevent curing.

Specimens of each analysis method are then removed from cold storage at the same time, and cured under with the same time-temperature conditions while measuring the corresponding properties. This ensures the two specimens have, as much as possible, identical, thermal histories,

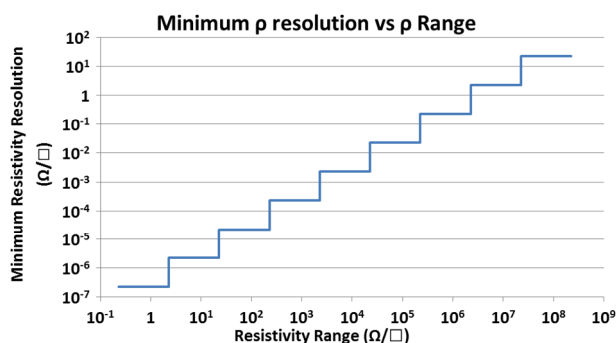


Figure 3 - Plot of the resistivity range vs resolution when using a Keithley 2400 in auto-ranging 4-wires sense mode with the designed mold-probe.

chemistry and filler content, as well as filler dispersion. Specimens in cold storage can be tested under varying conditions, and interwoven with other compositions, to investigate the full range of behaviour.

## RESULTS

The results of a typical experiment are shown in Figures 4 and 5, with conversion and heat capacity calculated from DSC data in figure 5a and the developed resistance behaviour in Figure 5b.

This set of demonstration tests revealed some unexpected behavior in the final stages of curing. As expected, the resistance initially begins to drop, around 40% conversion, approximately at 70°C. This corresponds with the beginning of the epoxy's contraction and solidification process, and is likely very close to the onset of gelation, though separate measurements are needed<sup>22</sup>.

The unexpected behavior comes around 90% conversion and 80°C, when the resistance begins to climb back to above the maximum detection range of the device. By approximately 100°C and 90% cured the material is fully insulating again. Then, in the last 1% of cure, starting at approximately 130°C, the resistance then sharply drops again, producing the final resistance value of the composite.

This is contrary to the expected pseudo-power law behavior that is typically reported and expected in the literature, which has been represented in Figure 5b by a dotted line that has been arbitrarily fit to the observed beginning and end resistances<sup>8</sup>. Instead, this high-conversion temporary resistance peak appears to be a newly observed behavior. The data presented in figure 5 is the average of 3 replicates, and so it is likely that this is a real process, and not a temporary failure in data collection. This leaves the possibility of either an inherent fault in the operation of the equipment, or real behavior produced by the cure of the composite. If it were real behavior by the composite, we would expect there to be additional physical phenomena associated with it.

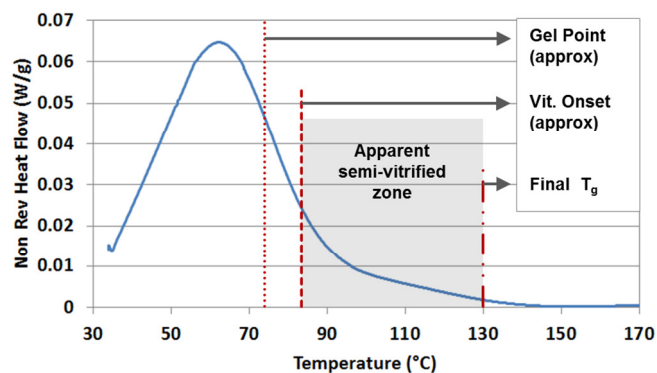


Figure 4 - Heat flow of exothermic cure of composite in MTDSC under continuous heating conditions. Note the shoulder on the high temperature side of the curve. Marked points are based on supplier data<sup>22</sup> and observed behavior.

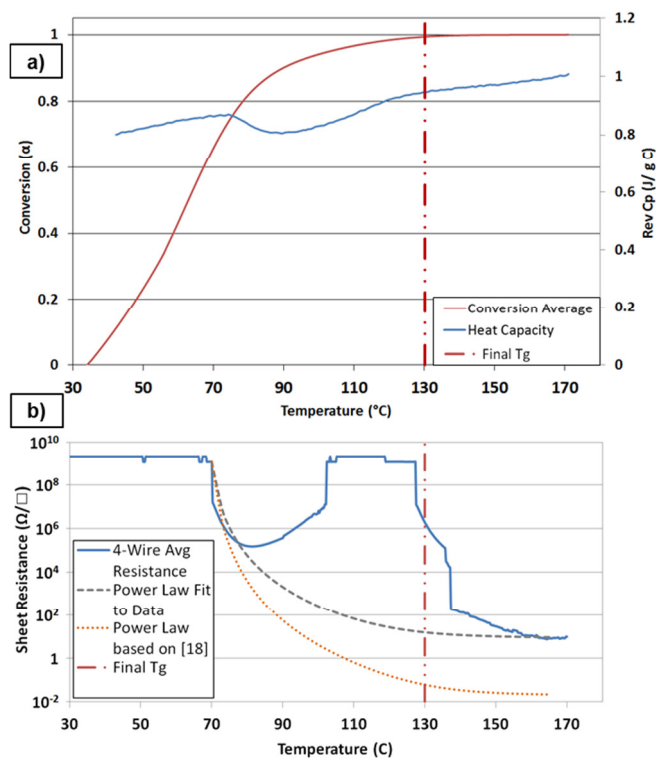


Figure 5 - a) Degree of conversion and reversing heat capacity component from MTDSC during continuous heating. b) correlated resistance of specimen (solid), under the same heating conditions. The grey dotted line is a representation of the expected power-law reduction, based on the experimentally obtained start and end points, and intended only as a conceptual guide. Orange is the same, based on regerence data<sup>18</sup>. Double-dot-dash line represents the final Tg, as measured during second heating.

A suggested source of systematic error is a temporary loss of connectivity between the composite and Teflon mold due to the contraction of the composite and the thermal expansion of the Teflon. In theory this relative contraction of the specimen might cause the contact pins to break their connection at partial cure, due to the developed tension. However, this is unlikely for several reasons. First, DGEBA resins are known to have a low cure-shrinkage, typically only of 4% - 6% density increase over the total cure. This corresponds to only approximately 1.5% linear contraction over the entire cure, if we assume that proportions are conserved. This would equate to a contraction of only 142 microns across the span between gold pins. Also, this is a conservative over-estimate since a substantial fraction of this contraction would have occurred prior to the gel-point, when the composite was still able to flow and redistribute. Therefore only contraction after the gel point would be likely to be capable of causing actual linear contraction perpendicular to the contact pins. However, more significant, after the experiment the specimen is removed from the mold by pressing the pins out of the contact terminals through the “troubleshooting port” seen in Figure 1c, at which point the specimens were removed with the gold pins still adhered and embedded

inside the sample, as seen in Figure 2a. Therefore it is highly unlikely for this to be the source of the unexpected resistance peak.

Not shown here, data was also analyzed when the source-meter and probe-mold continued to monitor the resistance during a cooling cycle and a subsequent second heating and cooling. During modulated second heating the DSC determined the ultimate glass transition of the composite, which was 130°C. Throughout this cool-heat-cool process, the resistance of the composite would be expected to change due to thermal expansion of the composite. This was observed, but only corresponded to a 5% reduction in resistance between 170°C and room temperature, once the epoxy was fully cured. Therefore, the resistance displayed here is representative of the final results, and not skewed by the heating conditions.

The unexpected resistance peak corresponds to two features in the DSC trace, which we hypothesize are related. The first is a linear segment of the conversion, between 75°C / 78% and 125°C / 98%. This is produced by a shoulder on the DSC heat flow plot, seen in Figure 4. Over the same temperature range, we see a depression in the heat capacity trace. The expected behavior of the reversing specific heat capacity is to slowly rise as the curing epoxy crosslinks, which for the most part is happening. However, over the temperature range listed above, the reversing Cp reduces, then gradually rises again, eventually tracing a line that matches the projection of the path before the depressed region, meeting back up just below 130°C. According to polymer physics principles, a sigmoidal increase in Cp corresponds to the transition of gelled epoxy from glassy to rubbery or leathery, while the opposite is a sign of the transition from to a glassy state<sup>23</sup>. Therefore, the signals seen in the DSC are likely the result of the instantaneous glass transition temperature ( $T_{g0}$ ) rising with the progressing cure, and approaching the current composite temperature. This would have cause the composite to enter the beginnings of vitrification, throttling the cure rate. This is supported by the observation that this depressed heat capacity returns to normal around the ultimate glass transition temperature, when the material would return to being fully rubbery.

Therefore, due to the concurrence of the independently recorded thermal process and the unexpected peak in the observed sheet resistance, it seems likely that the use of this resistance mold-probe and the associated methodology has uncovered a previously unobserved behavior for cross-linking conductive adhesives. The precise mechanism is not known at this time, but there is substantial evidence that it is related to the behavior of the curing polymer matrix interacting with the test conditions.

Since the composite is undergoing a significant fraction of its cure during this second non-conductive regime, there is a concern that the solidifying polymer network will form in such a way that will prevent relaxation and complete

reconnection of the conductive filler network after the cure is complete. If so, the mechanisms underlying this resistance peak may be the cause of the final resistance of composites being dependent on the cure conditions and thermal history of the composite<sup>8</sup>. If vitrification, partial or otherwise, of the composite during cure influences the final developed resistance, there would be far-ranging implications of the industry standard methods used to pre-cure and post-cure conductive adhesives. If such is the case, this equipment and methodology would be significant for the investigation and optimization of such behaviors.

Similarly, the mechanisms related to this resistance peak are likely composition dependent. Since the unusual behaviour appears to be a polymer-driven process, controlling the polymer binder's properties, such as stiffness and ultimate glass transition temperature, may substantially alter the developed properties in unexpected ways. Applying this continuous in-situ measurement methodology to multi-heating rate cure kinetic studies may allow the development of detailed process maps, characterizing a composition's resistance behavior with respect to its conversion-time-temperature relationship.

Filler content and composition will also likely be significant independent factors: it is currently unknown on what scale this mechanism operates. For example, nanoparticles may be more strongly influenced due to their size, or below the length-scale that can be affected. In composites where sintering between adjoining nanoparticles is expected during cure, these fluctuations in the filler network conductivity may inhibit formation of conductive filler networks. Hybrid systems containing a mixture of nano- and micro- fillers would also be expected to behave differently, and varying the stiffness and aspect ratio of the fillers may alter the outcome. It has also been widely reported that nanofillers can raise or lower final T<sub>g</sub>, as can the solvents used to disperse them, which may lead to further sources of influence on this mid-cure resistance peak. The equipment and methodologies reported here are expected to be instrumental to investigating these complex behaviors, and allow the faster development and optimization of future nanocomposite conductive adhesives.

Further enhancements of the equipment may also be possible. Reducing thermal mass would allow for higher stable heating rates. The addition of a multiplex switcher would allow multiple specimens to be monitored at the same time in a group of molds, increasing experimental throughput. The top half of the mold could be modified to allow a DMA, or a Thermomechanical Analyzer (TMA), to monitor the mechanical properties during cure, post-gelation, using a glass or Teflon probe.

## CONCLUSION

To advance to the understanding of an under-investigated aspect of cure progression of thermosetting conductive composites, an electrical resistance-sensing mold has been developed and tested. Paired with calorimetry measurements

under the same heating conditions, a description of the developing conductivity throughout the cure conversion was obtained. Unexpected and previously unreported behavior was identified, which appears to be related to the interaction of the polymeric matrix and the conductive fillers. Further experimental work, using a variety of conditions and composite compositions will be needed to determine the details of this behavior, which is likely thermal history dependent, and may be important for optimizing the pre-cure-post-cure cure cycles often used in industry.

## ACKNOWLEDGEMENTS

The authors gratefully acknowledge financial support by the Refined Manufacturing Acceleration Process Network (ReMAP).

## REFERENCES

- 1 L. Fan, *et al.*, Int Symp. Adv. Pack. Matls., 2002.
- 2 B. M. Amoli, *et al.*, Zhao, Macromol Mater Eng., 2014, 299, 739.
- 3 H. Cui, *et al.*, Polym. Int. 62, 2013, 1644.
- 4 C.G.L. Khoo, *et al.*, Int. Electron. Pack. Conf., 1996, 483.
- 5 H.K. Kim, F.G. Shi, Microelectr J, 32, 4, 2001, 315.
- 6 D. Chen, *et al.*, J. Mater. Sci.: Mater. Electron. 21, 2010, 486.
- 7 Z.X. Zhang, *et al.*, J. Adhes. Sci. Technol. 25, 13, 2011.
- 8 M. Inoue, K. Suganuma, Solder. Surf. Mt. Tech., 18, 2, 2006, 40.
- 9 K. Pashayi, *et al.*, J Appl Phys., 111, 2012, 104310.
- 10 P. Peng, A. *et al.*, J Mater Chem., 22, 2012, 12997.
- 11 S.B. Sepulveda-Mora, S.G. Cloutier, J Nanomater., 2012, 286104.
- 12 J. Sopousek, *et al.*, J Min Metall Sect B-Metall., 48, 2012, 63.
- 13 J.A. Spechler, C.B. Arnold, Appl Phys A, 108, 2012, 25.
- 14 Y. Tao, *et al.*, Nanoscale Res Lett. 8, 2013, 147
- 15 D.P. Langley, *et al.*, Nanoscale, 6, 2014, 13535.
- 16 P. Peng, *et al.*, ACS Appl Mater Interfaces, 7, 2015, 12597.
- 17 H. Gao, *et al.*, Int. J. Polym. Mater., 2011, 60, 6, 409.
- 18 N. Xiong, *et al.*, Int. Conf. Electron. Pack. Tech., 2014.
- 19 Y.H. Wang, *et al.*, J. Mater. Sci.: Mater. Electron., 2015, 26, 2, 621.
- 20 Y.H. Wang, *et al.*, J. Mater. Sci.: Mater. Electron., 2015, 26, 10, 7927.
- 21 D.K. Schroder, Semiconductor Material and Device Characterization, 3rd Ed., Wiley, 2006.
- 22 Dow Chemical, D.E.R. 331 Liquid Epoxy Resin Product Information, Dow Chemical Company.
- 23 J. D. Menczel, R. B. Prime, Thermal analysis of Polymers, Fundamentals and Applications, Wiley, Hoboken, New Jersey, 2009, 58-80.